Genomic evidence reveals a radiation of placental mammals uninterrupted by the KPg boundary

Liang Liu[a,b,1], Jin Zhang[c,1], Frank E. Rheindt[d,1], Fumin Lei[e], Yanhua Qu[e], Yu Wang[f], Yu Zhang[f], Corwin Sullivan[g], Wenhui Nie[h], Jinhuan Wang[h], Fengtang Yang[i], Jinping Chen[j], Scott V. Edwards[a,k,2], Jin Meng[l], and Shaoyuan Wu[a,m,2]

[a]Jiangsu Key Laboratory of Phylogenomics and Comparative Genomics, School of Life Sciences, Jiangsu Normal University, Xuzhou 221116, Jiangsu, China; [b]Department of Statistics & Institute of Bioinformatics, University of Georgia, Athens, GA 30606; [c]Key Laboratory of High Performance Computing and Stochastic Information Processing of the Ministry of Education of China, Department of Computer Science, College of Mathematics and Computer Science, Hunan Normal University, Changsha, Hunan 410081, China; [d]Department of Biological Sciences, National University of Singapore, Singapore 117543; [e]Key Laboratory of Zoological Systematics and Evolution, Institute of Zoology, Chinese Academy of Sciences, Beijing 100101, China; [f]State Key Laboratory of Reproductive Biology & Institute of Zoology, Chinese Academy of Sciences, Beijing 100101, China; [g]Key Laboratory of Vertebrate Evolution and Human Origins of the Chinese Academy of Sciences, Institute of Vertebrate Paleontology and Paleoanthropology, Chinese Academy of Sciences, Beijing 100044, China; [h]State Key Laboratory of Genetic Resources and Evolution, Kunming Institute of Zoology, Chinese Academy of Sciences, Kunming, Yunnan 650223, China; [i]Wellcome Trust Sanger Institute, Wellcome Trust Genome Campus, Hinxton CB10 1SA, United Kingdom; [j]Guangdong Public Laboratory of Wild Animal Conservation and Utilization, Guangdong Key Laboratory of Integrated Pest Management in Agriculture, Guangdong Institute of Applied Biological Resources, Guangzhou 510260, China; [k]Department of Organismic and Evolutionary Biology & Museum of Comparative Zoology, Harvard University, Cambridge, MA 02138; [l]Division of Paleontology, American Museum of Natural History, New York, NY 10024; and [m]Department of Biochemistry and Molecular Biology, 2011 Collaborative Innovation Center of Tianjin for Medical Epigenetics, Tianjin Key Laboratory of Medical Epigenetics, School of Basic Medical Sciences, Tianjin Medical University, Tianjin 300070, China

Contributed by Scott V. Edwards, June 3, 2017 (sent for review October 17, 2016; reviewed by Zhe-Xi Luo, William J. Murphy, and Nicolas Salamin)

The timing of the diversification of placental mammals relative to the Cretaceous–Paleogene (KPg) boundary mass extinction remains highly controversial. In particular, there have been seemingly irreconcilable differences in the dating of the early placental radiation not only between fossil-based and molecular datasets but also among molecular datasets. To help resolve this discrepancy, we performed genome-scale analyses using 4,388 loci from 90 taxa, including representatives of all extant placental orders and transcriptome data from flying lemurs (Dermoptera) and pangolins (Pholidota). Depending on the gene partitioning scheme, molecular clock model, and genic deviation from molecular clock assumptions, extensive sensitivity analyses recovered widely varying diversification scenarios for placental mammals from a given gene set, ranging from a deep Cretaceous origin and diversification to a scenario spanning the KPg boundary, suggesting that the use of suboptimal molecular clock markers and methodologies is a major cause of controversies regarding placental diversification timing. We demonstrate that reconciliation between molecular and paleontological estimates of placental divergence times can be achieved using the appropriate clock model and gene partitioning scheme while accounting for the degree to which individual genes violate molecular clock assumptions. A birth-death-shift analysis suggests that placental mammals underwent a continuous radiation across the KPg boundary without apparent interruption by the mass extinction, paralleling a genus-level radiation of multituberculates and ecomorphological diversification of both multituberculates and therians. These findings suggest that the KPg catastrophe evidently played a limited role in placental diversification, which, instead, was likely a delayed response to the slightly earlier radiation of angiosperms.

molecular clock | data partitioning | species tree estimation | placental diversification timing | trans-KPg model

Mammalian evolution has been intensively studied and is relatively well understood compared with the evolution of other animal clades (1–6). Despite significant recent progress, however, fundamental aspects of the pattern and timing of mammalian diversification remain vigorously debated (1–7). One highly controversial issue is whether the diversification of placental mammals took place before or after the Cretaceous–Paleogene (KPg) boundary (~66 Ma), which marked the extinction of nonavian dinosaurs and many other Mesozoic vertebrates (8–16). Three main models have been proposed to characterize the evolutionary history of placental crown groups. The explosive model puts both the origin and intraordinal diversification of Placentalia shortly after the KPg boundary (13). By contrast, the long-fuse model posits a Cretaceous origin of Placentalia with intraordinal diversification shortly after the KPg boundary, and the short-fuse model places the origin and intraordinal diversification of Placentalia in the Cretaceous (13). Paleontological evidence supports the explosive model, because all modern lineages of crown-group placentals first appear in the fossil record after the KPg boundary (15, 16). Molecular analyses, in contrast, provide almost unanimous support for a pre-KPg origin of Placentalia, although they disagree on the timing of intraordinal diversification relative to the KPg boundary (3, 5, 8–10). The resolution of the discrepancy between molecular and fossil evidence has remained one of the most crucial issues in mammalian evolutionary research, because

Significance

We produced a genome-scale dataset from representatives of all placental mammal orders to infer diversification timing relative to the Cretaceous–Paleogene (KPg) boundary. Our sensitivity analyses show that divergence time estimates within placentals are considerably biased by the specific way in which a given dataset is processed. We examined the performance of various dating approaches using a comprehensive scheme of likelihood analyses and computational simulations, allowing us to identify the optimal molecular clock parameters, gene sets, and gene partitioning schemes for reliable dating. Based on the optimal methodology, we present a hypothesis of mammalian divergence timing that is more consistent with the fossil record than previous molecular clock reconstructions, suggesting that placental mammals underwent a continuous radiation across the KPg boundary.

Author contributions: L.L., S.V.E., and S.W. designed research; L.L., F.E.R., C.S., S.V.E., J.M., and S.W. performed research; L.L., J.Z., F.E.R., and S.W. analyzed data; F.L., Y.Q., Y.W., Y.Z., W.N., J.W., F.Y., and J.C. contributed new reagents/analytic tools; S.W. wrote the paper; and L.L., F.E.R., S.V.E., and J.M. contributed to the writing and discussion.

Reviewers: Z.-X.L., The University of Chicago; W.J.M., Texas A&M University; and N.S., University of Lausanne.

The authors declare no conflict of interest.

Data deposition: The sequence reported in this paper has been deposited in the DRYAD database (accession no. 10.5061/dryad.bp462), and the RNA-seq raw data of pangolin and flying lemur were deposited in GenBank (accession nos. SRX3014245 and SRX3014246).

[1]L.L., J.Z., and F.E.R. contributed equally to this work.

[2]To whom correspondence may be addressed. Email: shaoyuanwu@outlook.com or sedwards@fas.harvard.edu.

This article contains supporting information online at www.pnas.org/lookup/suppl/doi:10.1073/pnas.1616744114/-/DCSupplemental.

the severity of the end-Cretaceous mass extinction implies that pre-KPg and post-KPg diversification events would have taken place in radically different ecological contexts.

Successful molecular dating of divergence events depends on various factors, the most critical of which are a rigorous set of fossil calibration points, a reliable phylogenetic topology, and rigorous application of molecular clock methodologies (17, 18). However, fossil calibrations used previously have varied in both number and quality (19, 20), and several important features of the mammalian phylogenetic tree remain unresolved despite considerable recent effort (1–4, 21–26). In addition, there has been limited assessment of the impact of different analytical parameters and clock models on dating estimates.

In this study, we applied multiple analytical strategies to a genome-scale dataset to resolve the placental mammalian tree. We calibrated the optimal tree recovered with 21 conservatively selected fossil constraints. To achieve reliable dating, we scrutinized molecular clock methodologies in detail, showing that gene partitioning schemes, clock models, and genic deviation from the assumptions of a molecular clock have a pronounced impact on dating placental divergence. Although we know that fossils are more important than extensive sequence data in achieving reliable dates (27), our large dataset allowed us to extensively explore the effect of diverse signals in the subsamples of our data on dating estimates. Our results suggest resolution of some major controversies in the mammalian tree and a hypothesis of placental diversification, termed the "trans-KPg model," which uniquely envisions the rise of placental orders as an uninterrupted radiation across the KPg boundary.

Results

A Placental Tree Based on Genome-Wide Data. We collected genome-scale DNA sequence data for 4,388 genes across 82 mammalian species, including transcriptome data from flying lemurs (Dermoptera) and pangolins (Pholidota). Our taxon sampling includes all 20 traditionally recognized extant placental orders, as well as eight nonmammalian outgroup vertebrates (Dataset S1). Gene length averaged 2,972 bp (ranging from 500–7,995 bp), and the total aligned length of our concatenated data amounted to 13,040,111 bp. Each of the 4,388 alignments contains 81–90 species. The proportion of missing genes across the 90 taxa ranges from 0 to 15.7%, with an average of 4.17% (Datasets S2–S5). Recent phylogenomic research affirms a crucial role for among-lineage base compositional variation in achieving congruent results (28). In particular, the third codon position (C3) is characterized by strong base compositional bias and high substitution rates, and differs substantially in phylogenetic signal from the first and second codon positions (C12) (28). To address this issue, we divided our sequence data into three partitions: (*i*) C12, (*ii*) C3, and (*iii*) complete coding sequences (CDSs). For construction of species trees, we applied two coalescence methods, species tree estimation using average ranks of coalescence (STAR) and the neighbor-joining method for reconstructing unrooted species tree (NJst) (29, 30), which have been shown to be more robust than concatenation to the combined effects of incomplete lineage sorting and long-branch attraction (31), as well as a concatenation method as implemented in RAxML (32).

The two coalescence methods disagreed only in the positions of two nodes for C3, with neither set of alternative placements receiving high branch support (*SI Appendix*, Figs. S1–S4). Hence, we report only the STAR results below and refer to them simply as coalescence results. Regarding interrelationships among placental orders, coalescence results are much more congruent across the three codon partitions than concatenation results (*SI Appendix*, Figs. S3–S6). The C12 and CDS coalescence trees for placentals are identical at the interordinal level, whereas the C3 tree is divergent only in placing tenrecs as sister to all other Afrotheria rather than embedded within them [bootstrap percentage (BP) = 100; *SI Appendix*, Figs. S3 and S4].

The concatenation trees, by contrast, differ substantially from each other and from the coalescence trees. In concatenation trees, tenrecs are consistently placed as sister to golden moles (BP = 100), while the aardvark is placed basally within Afroinsectiphilia (BP = 100; *SI Appendix*, Figs. S5 and S6). Hyraxes and elephants are sister taxa in the concatenation trees (BP = 100 for C12, BP = 99 for CDS, and BP = 70 for C3), whereas elephants and sirenians are sister taxa in the coalescence trees (BP = 100; *SI Appendix*, Figs. S3–S6). The C12 and CDS concatenation trees recover Afrotheria as the most basal placentals (BP = 85 for C12, BP = 83 for CDS; *SI Appendix*, Fig. S6), whereas the C3 concatenation tree recovers a monophyletic Atlantogenata (Afrotheria + Xenarthra) in this position (BP = 100; *SI Appendix*, Fig. S5). Finally, Chiroptera are placed as sister to Cetartiodactyla in CDS (BP = 89) and C3 (BP = 97) concatenation trees, but in an alternative, relatively basal position within Laurasiatheria in the C12 concatenation tree (BP = 86; *SI Appendix*, Figs. S5 and S6).

Our results show that coalescence analysis generated nearly uniform results when applied to C12, C3, and CDS partitions, whereas concatenation analyses were affected by conflicting topologies pertaining to key placental nodes (e.g., root of placentals and relationships within Laurasiatheria), suggesting that coalescence methods are able to yield a more stable and consistent resolution of the placental tree than concatenation (2, 31). In addition, when comparing the performance of codon partitions, C3 yielded unusual topological arrangements in outgroup clades that were difficult to reconcile with basic biological insights (e.g., the coelacanth placement). For outgroup taxa, coalescence and concatenation methods both generated variable topologies across different codon partitions (*SI Appendix*, Figs. S3–S6). The C3 partition is particularly unusual in that coalescence analysis recovered a coelacanth-anuran clade as sister to Reptilia, whereas concatenation recovered coelacanths as closer to amniotes than anurans (*SI Appendix*, Figs. S3–S6), suggesting that C3 contained an unreliable phylogenetic signal at the level of outgroup relationships. In contrast, C12 produced expected branching patterns with regard to these well-understood outgroup taxa. When codons were analyzed unpartitioned (i.e., CDS), results were largely intermediate between C12 and C3. These results indicate that C12 contained the most reliable signal in our genomic dataset, suggesting that coalescence analysis of C12 represents an optimal approach to resolving placental phylogeny. Hence, we consider the C12 coalescence tree the most reliable topology obtained in our analyses (Fig. 1 and *SI Appendix*, Fig. S3*A*).

Our coalescence tree supports and further refines a large body of previous phylogenetic work on placental phylogeny (2, 3, 6, 11, 21, 33) (Fig. 1 and *SI Appendix*, Fig. S3*A*). For instance, regarding the controversial basal arrangement of placentals, our analysis lends full support to a previous proposal to group Afrotheria and Xenarthra into Atlantogenata, which, in turn, is sister to the remaining placentals (Laurasiatheria) (2, 7, 21). Interestingly, tree shrews, which are found to be most closely related to primates by some previous phylogenomic studies (2, 33), emerge as the sister of lagomorphs and rodents in our coalescence tree (BP = 100; *SI Appendix*, Fig. S3*A*). Similarly, perissodactyls are retrieved as the sister clade to cetartiodactyls with full support in our study, whereas previous phylogenomic work has aligned them closer to carnivores with high support (BP > 90) (2, 33).

Dating the Mammalian Tree. Our dating analysis was performed using MCMCTree (34–36) with 21 conservatively selected fossil calibrations. Compared with two major previous studies on mammalian evolution (3, 5), our set of fossil calibrations was older, on average, and more evenly distributed across time (*SI Appendix*, Fig. S7). Analyses were performed using the C12 dataset on the C12 STAR tree, our most robust topology. We removed 521 genes from dating

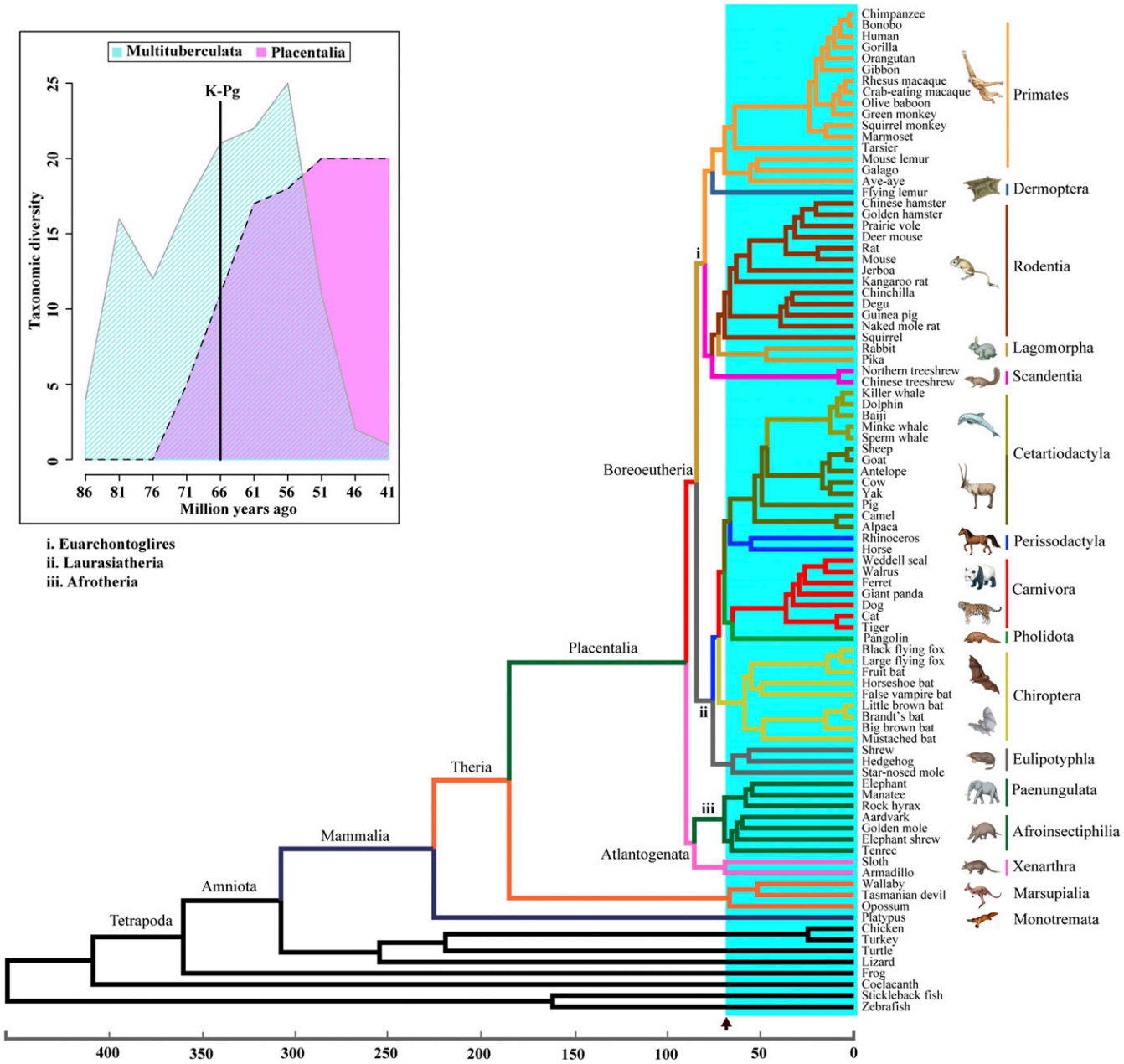

Fig. 1. Molecular time scale of mammalian diversification. A time tree calibrated under the IRM with single-gene partitions based on 200-gene sets from quintile 1 is shown, using a topology constructed from coalescence analysis of the C12 dataset and 21 fossil calibration points. The arrow indicates the KPg boundary at 66 Ma, and shading indicates the Cenozoic era. (*Inset*) Increasing ordinal-level diversity of placentals (purple) and genus-level diversity of multituberculate mammals (blue) during the Late Cretaceous and early Cenozoic. The data on multituberculate diversity are based on a study by Wilson et al. (56).

analysis either because their sequences were absent for two outgroup taxa (zebrafish and stickleback) or because they compromised MCMCTree computations. As a result, a total of 3,867 genes were retained for dating analysis.

Previous applications of molecular clocks suggest that dating analyses may be prone to a host of biases (37, 38). Therefore, we rigorously examined our sequence data using a range of analytical and subsampling schemes to detect potential biases (39). First, to examine the effects of genic deviation from the assumptions of a molecular clock, we devised a parameter to quantify the degree of violation of a molecular clock (DVMC) based on the SD of branch lengths for each gene tree. We divided all 3,867 genes into five quintiles from the lowest to highest DVMC, with each quintile containing 773/774 genes. Bayesian analyses of such large gene sets became computationally intractable on our large taxon set. Therefore, and additionally to examine the effects of stochastic subsampling of genes and gene partitioning schemes (39), we sampled three random gene sets of 60, 100, and 200 genes, respectively, for each quintile, resulting in nine gene sets per quintile. Each gene set was then subjected to five partitioning schemes: a single partition (p1), 5 partitions (p5), 10 partitions (p10), 20 partitions (p20), and every gene as a separate partition (p60, p100, and p200, respectively). All p5 partitions contained the same number of genes within a gene set, as did all p10 and p20 partitions. Lastly, each gene set was analyzed using both the autocorrelated rates model (ACRM) and the independent rates model (IRM) to account for model-related differences in dating estimates (40, 41). Loci across the five

quintiles broadly resembled each other in their proportion of variable sites (*SI Appendix*, Fig. S8), although loci with the lowest deviation from molecular clock assumptions (i.e., those in quintile 1) had a somewhat lower average proportion of variable sites (~0.416) than loci from the other four quintiles (0.482–0.528). In addition, loci from quintile 1 exhibited a smaller variance in the proportion of variable sites across loci compared with loci from the other four quintiles (*SI Appendix*, Fig. S8), suggesting that the loci in quintile 1 are characterized by the lowest degree of heterogeneity in absolute branch lengths of gene trees.

Reassuringly, random subsampling of all 3,867 genes had no significant impact on the dating of divergence events both within and among resampled sets of 60, 100, and 200 genes (*SI Appendix*, Fig. S9). Therefore, all subsequent results are reported on the basis of the 200-gene sets. When comparing results across partitioning schemes ranging from p1 to p200, average estimates of placental node ages appeared to increase with an increased number of gene partitions under the ACRM (Fig. 2*A* and *SI Appendix*, Fig. S10). In contrast, under the IRM, average divergence estimates were generally reduced by an increased number of gene partitions (Fig. 2*A* and *SI Appendix*, Fig. S11). When examining the effects of DVMC

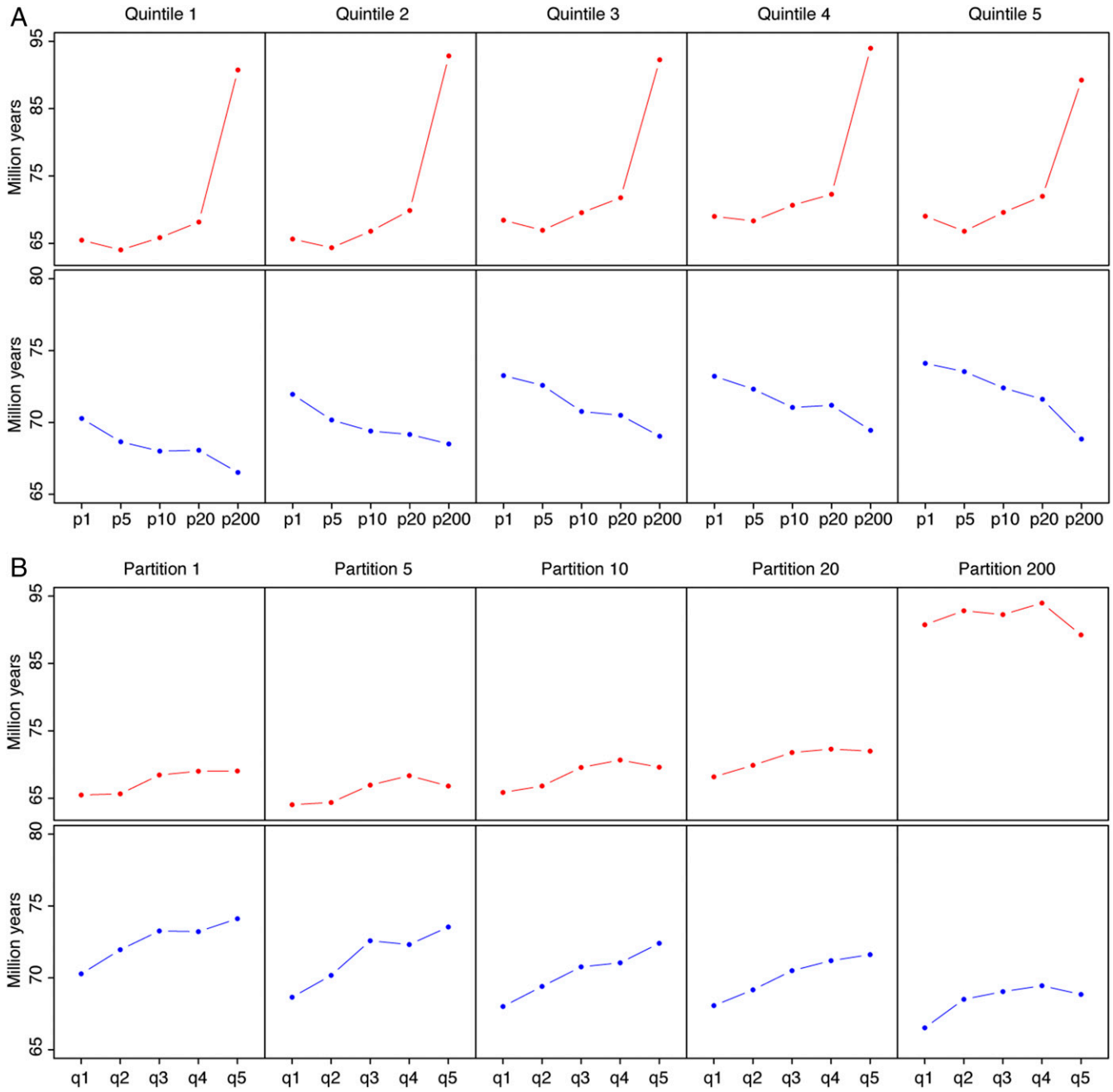

Fig. 2. Comparison of average age estimates for placental orders across clock models, gene partitioning schemes, and DVMC assumptions. (*A*) Age estimates averaged across all 20 placental orders calculated from 200-gene sets across partitions. (*B*) Age estimates averaged across all 20 placental orders calculated from 200-gene sets across quintiles (from lowest to highest DVMC). Note that q1 to q5 refer to quintiles 1–5. The red color indicates age estimates calculated under the ACRM, and the blue color indicates age estimates calculated under the IRM.

on molecular dating, we found that genes with a lower DVMC generally yielded younger nodal estimates across placentals than genes with a greater violation of the clock. This trend held true for both the ACRM and IRM (Fig. 2*B* and *SI Appendix*, Figs. S10 and S11).

To examine the effects of alternative topologies on dating, we used one 200-gene set from the first quintile across all five partitioning schemes to perform analyses based on the topology of the C12 concatenation tree. This tree differs from the C12 coalescence tree in arrangements at the placental root and within Afrotheria. Because one of our 21 calibrations related to a node (i.e., Tethytheria) that had not been retrieved by this concatenation tree, we reduced the number of calibrations to 20. The results showed minor differences in nodal dating compared with those estimated from the coalescence tree, further strengthening confidence in the timing of placental diversification as revealed by our study (*SI Appendix*, Fig. S12).

None of our dating results supported the explosive model of placental diversification (*SI Appendix*, Figs. S10 and S11). Generally, we found that the short-fuse model was supported by 10% of our analytical combinations (i.e., those in which the ACRM was applied on single-gene partitions under all DVMC levels), whereas dating estimates from gene sets with high DVMC levels under the IRM (using p1 and p5), which accounted for 8% of our analytical combinations, were roughly consistent with the long-fuse model. The remaining 82% of combinations of gene partitions and DVMC levels under both the ACRM and IRM are generally consistent with a model of diversification that we termed the trans-KPg model of placental diversification (*SI Appendix*, Figs. S10 and S11). These results indicate that clock models, partitioning schemes, and DVMC levels strongly influence dating outcomes, and suggest that an evaluation of these parameters is an important part of accurate dating of placental diversification (28).

Assessment of Molecular Clock Models. Our data indicate that partitioning schemes and DVMC classes can considerably affect dating estimates, and that this impact can be different across partitioning schemes depending on which clock model is chosen. Hence, we examined the likelihood space between the two models under different partitioning schemes and DVMC classes to determine which model is more appropriate for dating placental divergence.

We first calculated Bayes factors (BFs) based on the log-likelihood values produced by MCMCTree across partitioning schemes and DVMC classes. Because the method uses approximate likelihood scores that are comparable only across the same data types, we compared likelihood scores and BFs between the IRM and ACRM only across equal partitioning schemes with the same data. The BF analyses strongly favor the IRM over the ACRM for all partitioning schemes and DVMC classes, except for p1 (*SI Appendix*, Table S1). The calculation of BFs is based on the harmonic mean of the difference of marginal likelihoods of the two models, which has a wide variance. Therefore, even though the two models seem to perform similarly under p1, we cannot rule out that one model still outperforms the other. When plotting log-likelihood scores across iterations for each model under different partitioning schemes and DVMC quintiles, we again found that the IRM outperforms the ACRM, except for p1 (*SI Appendix*, Fig. S13). For all partitions other than p1, the magnitude of the BF favoring the IRM makes it unlikely that other methods for assessing BFs, such as thermodynamic integration (42), would yield a different result.

To compare the IRM and ACRM further, we used simulations to assess goodness of fit of the two models to empirical data. We simulated gene trees under both models, and compared the distributions of average branch lengths across simulated gene trees with the distribution of average branch lengths estimated from the empirical data. The results show that across partitioning schemes and DVMC classes, the IRM consistently generates branch lengths that closely correspond to those derived from the empirical data, whereas the ACRM produces branch lengths that considerably deviate from the empirical values and exhibit a much wider variance (Fig. 3 and *SI Appendix*, Fig. S14). In summary, our simulations, BFs, and likelihood-based analyses consistently support the conclusion that the IRM is preferable over the ACRM in dating placental divergence.

Selection of Optimal Partitioning Schemes and DVMC Classes. We carried out simulations to assess the impact of DVMC and gene partitioning scheme on the reliability of dating estimates under the IRM. We simulated DNA sequence data from two time trees estimated from the empirical 200-gene sets that deviated strongly from one another in their implications for ordinal divergences, with one reflecting the youngest estimates for placental divergence estimated from the 200-gene sets under the IRM, a scenario akin to a trans-KPg radiation of placentals ("shallow tree"), and the other reflecting the oldest estimates, which are roughly consistent with a long-fuse model ("deep tree"). To examine the effects of DVMC levels on dating estimates, sequence data were simulated from each of the two time trees under the IRM with (*i*) no deviation from molecular clock assumptions, (*ii*), a baseline level of DVMC (based on the rate variance σ^2 corresponding to each of the two time trees), (*iii*) a high level of DVMC (based on an increase of 1 in the rate variance σ^2 from baseline-DVMC simulations), and (*iv*) an intermediate level of DVMC (based on an increase of 0.5 in the rate variance σ^2 from baseline-DVMC simulations). We simulated three replicates for each combination of DVMC classes and the two time trees. Our

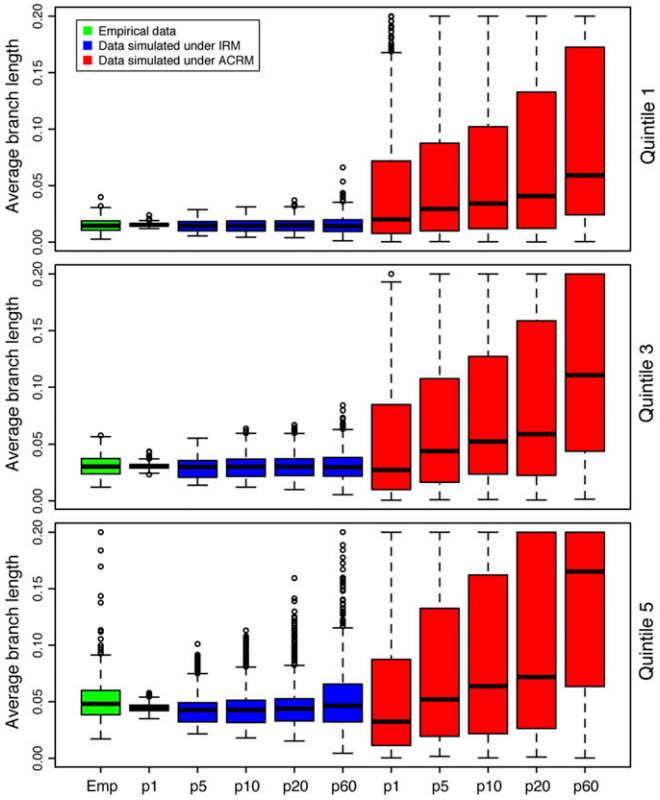

Fig. 3. Comparison of the distribution of branch length estimates across gene partitioning schemes and quintiles of varying levels of deviation from molecular clock assumptions between simulated and empirical gene trees. Note that average branch length values greater than 0.2 are truncated because wide variances of some partitions under the ACRM render full visualization difficult. Emp, empirical data.

simulations show that an increased number of gene partitions under deviation from molecular clock assumptions leads to a reduction of estimation error in divergence dating, with the best outcomes under single-gene partitions. Conversely, arrangements in which all genes are united into one partition invariably produce the poorest estimates (*SI Appendix*, Fig. S15). These analyses also indicate that genic deviation from the assumptions of a molecular clock have a considerable impact on dating outcomes, because the estimation error is positively correlated with rising values of DVMC (*SI Appendix*, Fig. S15). In contrast, scenarios with no deviation from molecular clock assumptions consistently yield the least amount of estimation error regardless of data partitioning scheme, with a single exception relating to an elevated estimation error in the shallow tree when all loci are combined into a single partition (*SI Appendix*, Fig. S15).

Lineage-Through-Time Analysis. We applied the birth-death-shift model of Stadler (43) to assess the importance of the KPg boundary extinction event on the diversification pattern of placental mammals. We ran the maximum likelihood method implemented in the R package TreePar (43), fitting the optimal time tree (*Results*) to models with no, one, two, and three rate shifts multiple times and estimating rates in a grid of 0.1-My steps between 2 and 200 Ma (43). Using a likelihood ratio test, the models with no shift and one shift in diversification rate were rejected ($P < 0.05$; *SI Appendix*, Table S2), but a model with two shifts in diversification rate was not ($P > 0.05$; *SI Appendix*, Table S2). Thus, the likelihood ratio test favors a model with two shifts in diversification rate occurring at 54 Ma (slowdown in diversification rate) and 88 Ma (increase in rate) (*SI Appendix*, Table S3), but not around the KPg boundary extinction event at ∼66 Ma (Fig. 4). Additionally, our analysis suggests a fairly constant rate of lineage turnover in our dataset (Fig. 4*B*).

Discussion

The coalescent tree based on the first and second codon positions (C12) provides strong resolution of a number of mammalian relationships that have long been controversial (7) (Fig. 1 and *SI Appendix*, Fig. S3*A*), and refines an earlier analysis based on less than 10% of the number of loci used in this study (2). It furnishes strong support for a basal division of placentals into Atlantogenata (Afrotheria and Xenarthra) and Boreoeutheria (Euarchontoglires and Laurasiatheria), and suggests many previously uncertain relationships within Laurasiatheria, Euarchontoglires, and Afrotheria (2, 21). Placement of Dermoptera as sister to primates, and Scandentia as sister to Glires, agrees with some previous phylogenetic proposals, but removes scandentians from their long-standing position as close primate precursors (1). The analysis upholds the monophyly of ungulates, which has been controversial, and posits a monophyletic Ferae (a clade uniting pangolins with carnivores) followed by Chiroptera as successive sister taxa to Ungulata. Previous studies that have, like the present analysis, found Afrotheria to be divided into Paenungulata and Afroinsectiphilia have tended to disagree on the internal topologies of major afrotherian clades (1, 3, 44, 45). Our results establish Tethytheria (a clade uniting elephants with manatees) as a monophyletic group within Paenungulata, hinting at a possible semiaquatic common ancestry for elephants and sirenians (46). Within Afroinsectiphilia, the fossorial Tubulidentata (aardvarks) and Chrysochloridae (golden moles) are recovered as sister taxa, with elephant shrews and tenrecs as successive outgroups. Exploring the impact of more complex substitution models and using noncoding markers on mammalian phylogenies are possible avenues for future work in mammalian phylogenetics (47). Additionally, the coalescent and subsampling methods we use here, while powerful and able to handle large datasets, are ultimately less accurate than a fully Bayesian approach (48); thus, improving Bayesian analyses to handle large datasets must be a priority for phylogenomics.

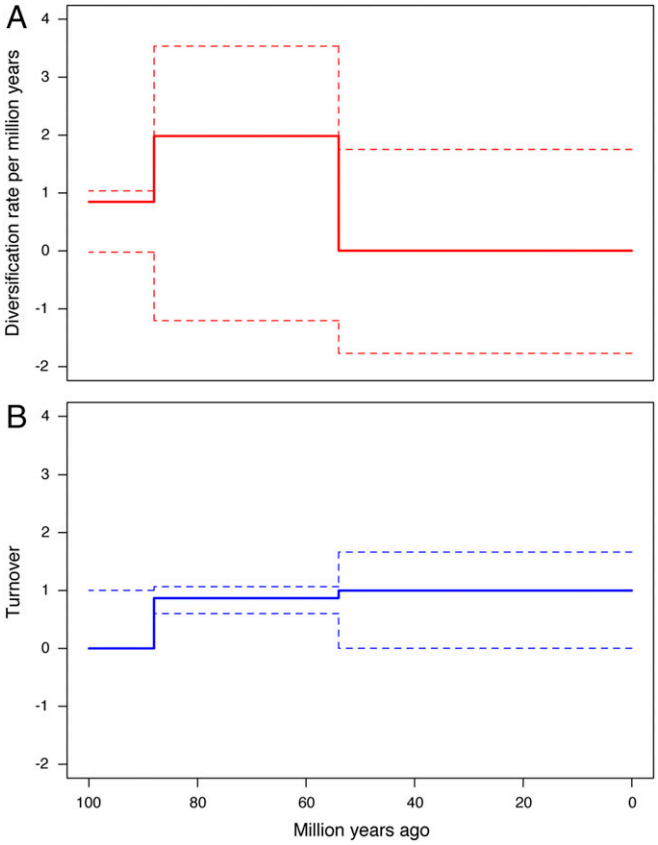

Fig. 4. Maximum likelihood estimates of diversification rates ($\lambda_i - \mu_i$) and turnover (λ_i/μ_i) for the mammalian phylogeny. (*A*) Diversification rate (speciation rate − extinction rate per million years) over time. (*B*) Turnover (extinction rate/speciation rate per million years) over time. The dashed lines are 95% confidence intervals.

Timing of Placental Divergence and the Trans-KPg Model. One of the greatest controversies surrounding the evolution of placental mammals relates to timing, especially with respect to the KPg extinction event (8, 12–14). This controversy appears to be obstinately irreconcilable, because previous molecular clock studies have consistently produced results at odds with one another and with fossil evidence (3–6, 9–11, 15, 16). In this study, we demonstrate that this controversy stems at least partly from the use of suboptimal molecular clock methodologies. Results estimated from our empirical gene sets encompassed widely divergent timing scenarios ranging from a deep Cretaceous diversification of placental orders to one that spans the KPg boundary, depending on a combination of clock models, gene partitioning schemes, and DVMC classes (Fig. 2 and *SI Appendix*, Figs. S10 and S11). This wide range in timing estimates mirrors the discordant results of prior molecular clock studies and their underlying variability in analytical models and parameters. Our sensitivity analyses demonstrate that in dating estimates, the IRM outperforms the ACRM based on a comprehensive comparison using BFs, log-likelihood scores, and the empirical fit of simulated branch length distributions of gene trees (Fig. 3, *SI Appendix*, Figs. S13 and S14, and Dataset S2). As a consequence, we recommend IRM-based analyses as the most robust methodology in dating placental divergence events when using MCMCTree (34). Furthermore, we performed simulations to assess the impact of partitioning schemes and DVMC classes on dating estimates, demonstrating that genes with a lower level of DVMC produce more reliable dating estimates than genes that strongly depart from molecular clock assumptions (*SI Appendix*, Fig. S15). When applying the IRM, our analyses also

underscore the importance of treating each gene as a separate partition, while attesting to poor performance using schemes that unite multiple genes into a single partition (*SI Appendix*, Fig. S15). These analyses suggest that the best dating outcome for placental mammals is produced by the application of an IRM with single-gene partitions based on genes with the lowest DVMC (Fig. 5*A* and *SI Appendix*, Fig. S11).

Our study presents a robust dating estimate for placental divergence that is rigorously tested using genome-scale sequence data. Although we know that accurate fossil calibration is more important for dating than more sequence data (27), our large dataset nonetheless allowed us to subsample our data and conduct extensive sensitivity analyses, which would not have been possible with a smaller dataset. Additionally, by examining the effect of variation in rates among genes and lineages on our dating estimates, with both empirical analyses and simulations, we show that relaxed clock methods are sensitive to rate variation among genes and lineages, and that the extent of clocklike evolution of the genes used for analysis can influence the results. Although our dating analysis did not incorporate uncertainty in the phylogenetic placement of fossils (49–51), we did scrutinize our fossils extensively and used only those with firm identifications and phylogenetic affinities.

Our dating estimates differ substantially from previous molecular clock-based estimates (Fig. 5); however, in many aspects, they are more congruent with the fossil record, significantly reducing, if not completely aligning, long-standing discrepancies in molecular and fossil dating (Figs. 1 and 5). In positing early Cenozoic origins for around half of placental orders, combined with intraordinal diversification taking place after the KPg boundary, our results do not correspond to any of the three existing models (long-fuse, short-fuse, and explosive) of placental diversification as originally defined (13); instead, they suggest a trans-KPg model: The diversification of placental orders began in the Late Cretaceous (~75.2 Ma), continued without apparent interruption across the KPg boundary, and ended in the early Cenozoic (~55.3 Ma), while intraordinal diversification followed rapidly in the early Cenozoic (Figs. 1 and 5). Our lineage-through-time analysis, which is consistent with analyses of previous studies (43), corroborated a lack of noticeable diversification rate shifts around the KPg boundary, further cementing a picture of early placental diversification in which the KPg boundary extinction event does not feature prominently (Fig. 4). It is worth noting that our hypothesis of placental diversification timing is not proposed on the basis of a single analysis under optimal criteria, but is consistent with 82% of all our IRM and ACRM analyses. Thus, our results do not depend on one specific dataset or analysis that we conducted, but were yielded by many analyses and datasets. We note that several nodes resulted in dating estimates under the optimal criteria that are seemingly in conflict with the fossil record (52). For example, the dating estimates for the divergence between northern tree shrews and Chinese tree shrews and for the base of Cetacea penetrated beyond the minimum bounds suggested by fossils, thereby resulting in younger molecular clock divergences, a potential issue of "zombie lineages" (53). Whether these outcomes are due to errors in clock methodology or the unreliability surrounding the fossil record is a topic for further study (54).

A recently proposed "soft explosive model," proposed not on the basis of empirical data but on a literature review, posits that an unspecified but low number of placental orders originated before the KPg boundary, while most originated afterward (55). This soft explosive model is evolutionarily different from our trans-KPg model in that it puts forth an explosive radiation, soft or otherwise, after the KPg boundary, in the same vein as the traditional explosive model. By contrast, the trans-KPg model envisages a steady diversification mode, with interordinal divergences in early placentals almost evenly spread on either side of the KPg boundary (Fig. 5*A*), resulting in no signal of "explosion." The lack of any signal of extinction or diversification of the KPg catastrophe in our analysis accentuates the distinction between the soft explosive model and our trans-KPg model.

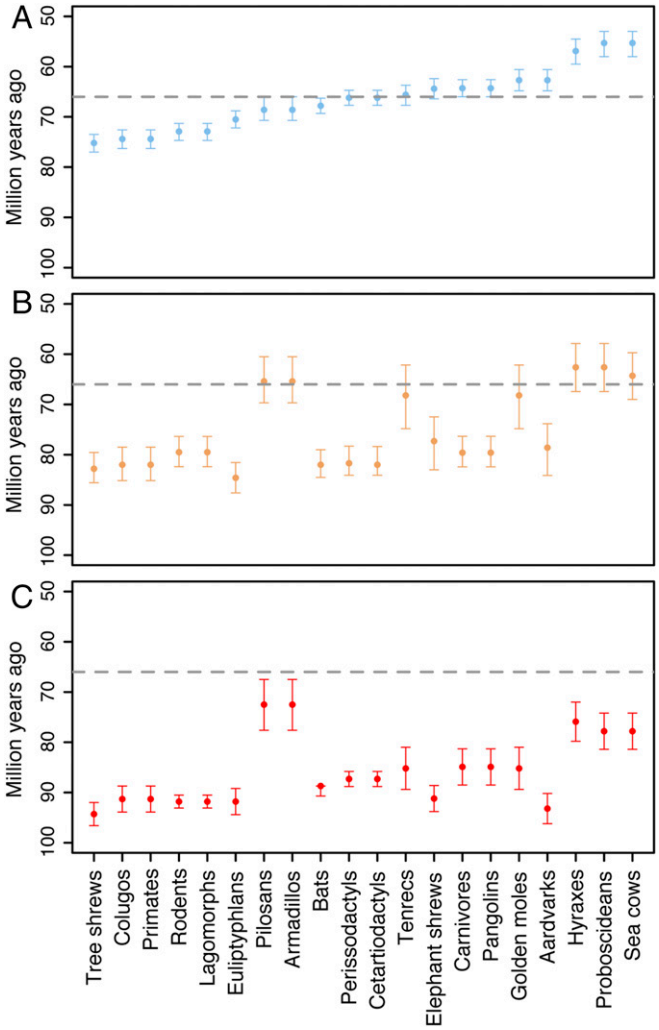

Fig. 5. Age estimates (with means and 95% confidence intervals) of interordinal divergence for all extant placental orders compared in this study and two major previous studies. (*A*) Diversification timing estimated in this study based on the optimal molecular clock methodology. (*B*) Diversification timing estimated by Meredith et al. (3), which is roughly consistent with the long-fuse model. (*C*) Diversification timing estimated by Bininda-Emonds et al. (5), which is generally consistent with the short-fuse model.

Ecology of Placental Diversification. The ordinal diversification of placentals in the Late Cretaceous and early Paleogene coincided with a genus-level radiation of multituberculates, a major clade of small Mesozoic mammals that also extended across the KPg boundary (56) (Fig. 1, *Inset*). Multituberculates appear to have shifted toward increased generic diversity, body size, and herbivory, and their diversification may have been a delayed response to the increasing dominance of angiosperms in Late Cretaceous floras (56). Most early placentals were likely insectivorous rather than herbivorous, but would have encountered new ecological opportunities as a result of the proliferation of insect herbivores and pollinators that undoubtedly accompanied the rise of angiosperms (57). For the crown therian clade that includes metatherians and eutherians and their relatives, there is also a gradual rise in ecomorphological disparity at the genus level during the Late Cretaceous and through the KPg boundary

(56, 58). This mirrors the diversification patterns of multituberculates, and the placental taxa (56, 58).

The KPg extinction was evidently a less critical event in mammalian history than has sometimes been supposed: At least two major mammalian groups radiated across the boundary with little interruption (Fig. 1, *Inset*). However, the intraordinal diversification of placental mammals appears to have been a Cenozoic phenomenon, consistent with the traditional view that mammals benefited from numerous vacant niches following the catastrophe (4). Molecular evidence from extant clades of placental mammals and paleontological evidence from multituberculates and nonplacental therians produce a coherent picture of mammalian diversification across the KPg boundary.

Materials and Methods

Estimation of Gene Trees. Maximum likelihood and bootstrap gene trees were estimated for CDS, C12, and C3, respectively. For each dataset, individual gene trees were estimated using the program PhyML (v3.0) (59) with its own best-fit substitution model selected by jModelTest (60, 61). The bootstrap analysis was performed with 100 bootstrap replicates for each of the 4,388 genes.

Concatenation Analysis of Species Trees. We conducted maximum likelihood estimates of species trees using the program RAxML (v8.0.22) (32) for concatenated sequences of the C12, C3, and CDS datasets, respectively. The maximum likelihood analyses of species trees were bootstrapped for 100 replicates based on an unpartitioned GTRCAT model. Because of the enormous computational demands of our analyses, we used the GTRCAT model for maximum likelihood analyses of the concatenated sequences based on the developers' recommendations for massive datasets. GTRCAT approximation can effectively accelerate computations on datasets with >50 taxa.

Coalescent Analysis of Species Trees. We conducted coalescent analysis of species trees using two recently developed coalescent methods: STAR (29) and NJst (30). For each dataset, the bootstrap gene trees were rooted by a single outgroup. Depending on presence or absence, the most remote outgroup taxon was chosen in the following order: zebrafish, stickleback, coelacanth, frog, lizard, and turtle. We then generated 100 bootstrap files for species tree estimation. The trees in the *i*th bootstrap file were the *i*th bootstrap trees across 4,388 genes. Thus, each bootstrap file contained 4,388 rooted bootstrap gene trees. For each bootstrap file of 4,388 rooted bootstrap gene trees, we estimated the species tree using STAR and NJst. We built a majority-rule consensus tree for 100 estimated species trees using PHYLIP v3.69 (62, 63).

Molecular Dating Analysis. We conducted Bayesian dating analyses using the program MCMCTree (34) as implemented in the PAML package (v4.8) (35, 36). Dating analyses were performed using the C12 dataset on both the C12 STAR and concatenation trees.

For the dating analysis, we removed 364 genes from the 4,388-gene dataset because they were not available for either of the two outgroup taxa appearing in the species tree (zebrafish and stickleback). A further 157 genes were additionally removed from the dating analysis because the MCMCTree program was unable to process them without fatal interruptions. As a result, 3,867 genes were retained for dating analysis (Dataset S6).

We estimated branch lengths for each gene using PhyML (v3.0) (59) with the Hasegawa, Kishino, and Yano (HKY) + GAMMA model, because MCMCTree allows for the use of HKY but not the generalized time-reversible (GTR) model. The average branch length of gene trees was used as a proxy of the overall mutation rate of each gene (9). In addition, estimated branch lengths were used to measure the DVMC for each gene. Considering a tree with N species, let x_i be the distance between the root of the tree and the species i (tip i of the tree). The DVMC was measured by the SD of x_i values [i.e., DVMC $= \sqrt{\frac{1}{N-1}\sum_{i=1}^{N}(x_i-\bar{x})^2}$].

We divided the 3,867 genes into five quintiles according to DVMC values, from the lowest to the highest. Each quintile comprises 773 or 774 genes, with the first quintile having the lowest DVMC values and the fifth quintile having the highest DVMC values. Given the large number of taxa and genes involved in dating analyses across different DVMC levels, the inclusion of all 773/774 loci from each quintile in MCMCTree runs was computationally intractable, because preliminary tests showed that a single MCMCTree run using 600 genes requires over a month to complete. Therefore, we resorted to a subsampling technique (39) in which we randomly drew 60, 100, and 200 genes from each quintile, and replicated this procedure three times for each of the three gene sets. As a result, a total of 45 subsets were analyzed in this study, with each quintile represented by nine subsets.

Further information on data collection, simulations, and fossil calibration points and additional details regarding molecular dating analyses are provided in *SI Appendix, SI Materials and Methods*.

ACKNOWLEDGMENTS. We thank Ziheng Yang and the three reviewers for their helpful comments, which substantially improved the quality of the manuscript. We thank S. Ho, W. Wang, Y. Deng, T. Sun, M. dos Reis, and M. Geng for technical assistance and Y. Xu for drawing Fig. 1. We thank the National Supercomputer Center at Tianjin, the Harvard University Research Computing Cluster, and the Georgia Advanced Computing Resource for computing support. This work was supported by funds from the Priority Academic Program Development of Jiangsu Higher Education Institutions, the National Natural Science Foundation of China (Grant 31470111 to S.W.), the startup funds from Jiangsu Normal University and Tianjin Medical University (to S.W.), and Hunan Provincial Education Department Fund Project (Grant 15K082 to J.Z.).

1. Asher RJ, Bennett N, Lehmann T (2009) The new framework for understanding placental mammal evolution. *BioEssays* 31:853–864.
2. Song S, Liu L, Edwards SV, Wu S (2012) Resolving conflict in eutherian mammal phylogeny using phylogenomics and the multispecies coalescent model. *Proc Natl Acad Sci USA* 109:14942–14947.
3. Meredith RW, et al. (2011) Impacts of the Cretaceous Terrestrial Revolution and KPg extinction on mammal diversification. *Science* 334:521–524.
4. O'Leary MA, et al. (2013) The placental mammal ancestor and the post-K-Pg radiation of placentals. *Science* 339:662–667.
5. Bininda-Emonds ORP, et al. (2007) The delayed rise of present-day mammals. *Nature* 446:507–512.
6. Murphy WJ, et al. (2001) Molecular phylogenetics and the origins of placental mammals. *Nature* 409:614–618.
7. Foley NM, Springer MS, Teeling EC (2016) Mammal madness: Is the mammal tree of life not yet resolved? *Philos Trans R Soc Lond B Biol Sci* 371:20150140.
8. dos Reis M, Donoghue PCJ, Yang Z (2014) Neither phylogenomic nor palaeontological data support a Palaeogene origin of placental mammals. *Biol Lett* 10:20131003.
9. dos Reis M, et al. (2012) Phylogenomic datasets provide both precision and accuracy in estimating the timescale of placental mammal phylogeny. *Proc Biol Sci* 279: 3491–3500.
10. Springer MS, Murphy WJ, Eizirik E, O'Brien SJ (2003) Placental mammal diversification and the Cretaceous-Tertiary boundary. *Proc Natl Acad Sci USA* 100:1056–1061.
11. Murphy WJ, et al. (2001) Resolution of the early placental mammal radiation using Bayesian phylogenetics. *Science* 294:2348–2351.
12. Bromham L, Penny D (2003) The modern molecular clock. *Nat Rev Genet* 4:216–224.
13. Archibald JD, Deutschman DH (2001) Quantitative analysis of the timing of origin of extant placental orders. *J Mamm Evol* 8:107–124.
14. Smith AB, Peterson KL (2002) Dating the time of origin of major clades: Molecular clocks and the fossil record. *Annu Rev Earth Planet Sci* 30:65–88.
15. Asher RJ, et al. (2005) Stem Lagomorpha and the antiquity of Glires. *Science* 307: 1091–1094.
16. Wible JR, Rougier GW, Novacek MJ, Asher RJ (2007) Cretaceous eutherians and Laurasian origin for placental mammals near the K/T boundary. *Nature* 447:1003–1006.
17. Arbogast B, Edwards SV, Wakeley J, Beerli P, Slowinski J (2002) Estimating divergence times from molecular data on phylogenetic and population genetic timescales. *Ann Rev Ecol Syst* 33.
18. Parham JF, et al. (2012) Best practices for justifying fossil calibrations. *Syst Biol* 61: 346–359.
19. Benton MJ, Donoghue MJ, Asher RJ (2009) Calibrating and constraining molecular clocks. *The Timetree of Life*, eds Hedges SB, Kumar S (Oxford Univ Press, Oxford), pp 35–86.
20. Wu S, et al. (2012) Molecular and paleontological evidence for a post-Cretaceous origin of rodents. *PLoS One* 7:e46445.
21. Murphy WJ, Pringle TH, Crider TA, Springer MS, Miller W (2007) Using genomic data to unravel the root of the placental mammal phylogeny. *Genome Res* 17:413–421.
22. Nikolaev S, et al.; NISC Comparative Sequencing Program (2007) Early history of mammals is elucidated with the ENCODE multiple species sequencing data. *PLoS Genet* 3:e2.
23. Wildman DE, et al. (2007) Genomics, biogeography, and the diversification of placental mammals. *Proc Natl Acad Sci USA* 104:14395–14400.
24. Prasad AB, Allard MW, Green ED; NISC Comparative Sequencing Program (2008) Confirming the phylogeny of mammals by use of large comparative sequence data sets. *Mol Biol Evol* 25:1795–1808.
25. Kriegs JO, et al. (2006) Retroposed elements as archives for the evolutionary history of placental mammals. *PLoS Biol* 4:e91.
26. Hallström BM, Kullberg M, Nilsson MA, Janke A (2007) Phylogenomic data analyses provide evidence that Xenarthra and Afrotheria are sister groups. *Mol Biol Evol* 24: 2059–2068.

27. Yang Z, Rannala B (2006) Bayesian estimation of species divergence times under a molecular clock using multiple fossil calibrations with soft bounds. *Mol Biol Evol* 23: 212–226.
28. Jarvis ED, et al. (2014) Whole-genome analyses resolve early branches in the tree of life of modern birds. *Science* 346:1320–1331.
29. Liu L, Yu L, Pearl DK, Edwards SV (2009) Estimating species phylogenies using coalescence times among sequences. *Syst Biol* 58:468–477.
30. Liu L, Yu L (2011) Estimating species trees from unrooted gene trees. *Syst Biol* 60: 661–667.
31. Liu L, Xi Z, Davis CC (2015) Coalescent methods are robust to the simultaneous effects of long branches and incomplete lineage sorting. *Mol Biol Evol* 32:791–805.
32. Stamatakis A (2006) RAxML-VI-HPC: Maximum likelihood-based phylogenetic analyses with thousands of taxa and mixed models. *Bioinformatics* 22:2688–2690.
33. McCormack JE, et al. (2012) Ultraconserved elements are novel phylogenomic markers that resolve placental mammal phylogeny when combined with species-tree analysis. *Genome Res* 22:746–754.
34. dos Reis M, Yang Z (2011) Approximate likelihood calculation on a phylogeny for Bayesian estimation of divergence times. *Mol Biol Evol* 28:2161–2172.
35. Yang Z (2007) PAML 4: Phylogenetic analysis by maximum likelihood. *Mol Biol Evol* 24:1586–1591.
36. Yang Z (1997) PAML: A program package for phylogenetic analysis by maximum likelihood. *Comput Appl Biosci* 13:555–556.
37. dos Reis M, et al. (2015) Uncertainty in the timing of origin of animals and the limits of precision in molecular timescales. *Curr Biol* 25:2939–2950.
38. dos Reis M, Donoghue PCJ, Yang Z (2016) Bayesian molecular clock dating of species divergences in the genomics era. *Nat Rev Genet* 17:71–80.
39. Edwards SV (2016) Phylogenomic subsampling: A brief review. *Zool Scr* 45:63–74.
40. Rannala B, Yang Z (2007) Inferring speciation times under an episodic molecular clock. *Syst Biol* 56:453–466.
41. Yang Z (2006) *Computational Molecular Evolution* (Oxford Univ Press, Oxford).
42. Lartillot N, Philippe H (2006) Computing Bayes factors using thermodynamic integration. *Syst Biol* 55:195–207.
43. Stadler T (2011) Mammalian phylogeny reveals recent diversification rate shifts. *Proc Natl Acad Sci USA* 108:6187–6192.
44. Arnason U, et al. (2008) Mitogenomic relationships of placental mammals and molecular estimates of their divergences. *Gene* 421:37–51.
45. Waddell PJ, Shelley S (2003) Evaluating placental inter-ordinal phylogenies with novel sequences including RAG1, gamma-fibrinogen, ND6, and mt-tRNA, plus MCMC-driven nucleotide, amino acid, and codon models. *Mol Phylogenet Evol* 28:197–224.
46. Andrews CW (1906) *A Descriptive Catalogue of the Tertiary Vertebrata of the Fayum, Egypt* (British Museum of Natural History, London).
47. Edwards SV, Cloutier A, Baker A (June 16, 2017) Conserved non-exonic elements: A novel class of marker for phylogenomics. *Syst Biol*, 10.1093/sysbio/syx058.
48. Xu B, Yang Z (2016) Challenges in species tree estimation under the multispecies coalescent model. *Genetics* 204:1353–1368.
49. Sauquet H, et al. (2012) Testing the impact of calibration on molecular divergence times using a fossil-rich group: The case of Nothofagus (Fagales). *Syst Biol* 61:289–313.
50. Zhang C, Stadler T, Klopfstein S, Heath TA, Ronquist F (2016) Total-evidence dating under the fossilized birth-death process. *Syst Biol* 65:228–249.
51. Ronquist F, Lartillot N, Phillips MJ (2016) Closing the gap between rocks and clocks using total-evidence dating. *Philos Trans R Soc Lond B Biol Sci* 371:20150136.
52. Emerling CA, Huynh HT, Nguyen MA, Meredith RW, Springer MS (2015) Spectral shifts of mammalian ultraviolet-sensitive pigments (short wavelength-sensitive opsin 1) are associated with eye length and photic niche evolution. *Proc Biol Sci* 282:20151817.
53. Springer MS, et al. (2017) Waking the undead: Implications of a soft explosive model for the timing of placental mammal diversification. *Mol Phylogenet Evol* 106:86–102.
54. Rannala B (2016) Conceptual issues in Bayesian divergence time estimation. *Philos Trans R Soc Lond B Biol Sci* 371:20150134.
55. Phillips MJ (2016) Geomolecular dating and the origin of placental mammals. *Syst Biol* 65:546–557.
56. Wilson GP, et al. (2012) Adaptive radiation of multituberculate mammals before the extinction of dinosaurs. *Nature* 483:457–460.
57. Moreau CS, Bell CD, Vila R, Archibald SB, Pierce NE (2006) Phylogeny of the ants: Diversification in the age of angiosperms. *Science* 312:101–104.
58. Grossnickle D, Newham E (2016) Therian mammals experience an ecomorphological radiation during the Late Cretaceous and selective extinction at the K-Pg boundary. *Proc R Soc B* 283:20160256.
59. Guindon S, et al. (2010) New algorithms and methods to estimate maximum-likelihood phylogenies: Assessing the performance of PhyML 3.0. *Syst Biol* 59:307–321.
60. Posada D (2008) jModelTest: Phylogenetic model averaging. *Mol Biol Evol* 25: 1253–1256.
61. Posada D, Crandall KA (1998) MODELTEST: Testing the model of DNA substitution. *Bioinformatics* 14:817–818.
62. Felsenstein J (1989) PHYLIP-Phylogeny Inference Package (Version 3.2). *Cladistics* 5: 164–166.
63. Margush T, McMorris FR (1981) Consensus n-trees. *Bull Math Biol* 43:239–244.